COMPARISON OF LOW-COST HANDHELD LIDAR-BASED SLAM SYSTEMS FOR MAPPING UNDERGROUND TUNNELS

P. Trybała [1,2], D. Kasza [2], J. Wajs [2], F. Remondino [1]

[1] 3D Optical Metrology (3DOM) unit, Bruno Kessler Foundation (FBK), Trento, Italy
Web: http://3dom.fbk.eu – Email: <ptrybala><remondino>@fbk.eu

[2] Department of Geodesy and Geoinformatics, Wrocław University of Science and Technology (WUST), Wrocław, Poland
Web: https://wggg.pwr.edu.pl/en/ – Email: <damian.kasza><jaroslaw.wajs>@pwr.edu.pl

Commission II

KEY WORDS: LiDAR SLAM, Low-Cost, Mobile Mapping, Open-Source, Underground Mining, Evaluation, Voxel

ABSTRACT:
The use of mobile mapping technologies (MMT) has become increasingly popular across various applications such as forestry, cultural heritage, mining, and civil engineering. While Simultaneous Localization and Mapping (SLAM) algorithms have greatly improved in recent years with regards to accuracy, robustness, and cooperativity, it is important to understand the limitations and strengths of each metrological measurement method to ensure the provision of 3D data of appropriate quality for the selected application. In this study, we perform a comparative analysis of three LiDAR-based handheld mobile mapping systems with survey-grade reference point clouds in a challenging test area of a partially collapsed underground tunnel. We investigate various aspects of 3D data quality, including accuracy and completeness, and present an improved method for 3D data completeness assessment aimed at evaluating SLAM-derived point clouds. The results demonstrate unique and diverse strengths and shortcomings of the tested mapping systems, which provide valuable guidelines for selecting an appropriate system for subterranean applications.

1. INTRODUCTION

Mobile mapping systems (Nocerino et al., 2019; Otero et al., 2020; Elhashash et al., 2022) are steadily growing in popularity for the 3D reconstruction of indoor spaces. They are becoming more and more available for end-users thanks to their simplicity in use and affordability. They can be a cost- and time-effective alternative for traditional methods such as photogrammetry or Terrestrial Laser Scanning (TLS) in particular for large areas where mobile acquisitions would speed-up the surveying operations. Handheld, backpack and robotic-based vision- (Menna et al., 2022; Perfetti and Fassi, 2022), LIDAR- (Liang et al., 2014; Xie et al., 2022) or hybrid- (Trybała et al., 2022) systems using SLAM (Simultaneous Localization and Mapping) are becoming widely applied in multiple fields, such as cultural heritage documentation (Di Stefano et al., 2021), forestry (Pierzchała et al., 2018) and mining (Jones, 2020; Ebadi et al., 2022). The application of mobile mapping technologies is quite complicated in underground, unstructured environments, since algorithms employed for motion estimation of the sensor have to deal with challenges such as low or uneven lighting, dust, high humidity, rough surfaces and overall lack of distinct visual and geometric features. Thus, a good understanding of the mapping system capabilities in terms of reliability and accuracy is needed for ensuring the compliance with the requirements of specific application. Moreover, in confined, underground spaces, multiple occlusions and a limited field of view of the sensors create other challenges for 3D data acquisition, leading to occurrences of holes and gaps in the resulting point clouds (Trybała et al., 2023).

1.1 Paper's aims

The goal of the work is to assess the quality (geometry compliance with respect to ground truth data) and completeness of 3D point clouds acquired with different handheld LiDAR-based SLAM solutions in unstructured underground conditions. A Livox- and Velodyne-based systems are benchmarked against a GeoSLAM ZEB Horizon and a TLS reference point cloud. For our analyses, different SLAM approaches are considered whereas a voxel-based point cloud comparison methodology is proposed, together with an improved method for evaluating the completeness of the 3D reconstruction.
The work is part of the EIT-RM project VOT3D which aims to support the raw material sector by introducing modern methods and innovative solutions for the optimization of underground ventilation in mining scenarios based on 3D data. Utilization of mobile mapping technologies in the subterranean conditions, despite constituting a challenge, is an important part of enabling realistic simulations of ventilation system operation in an industrial underground mine. Consequently, understanding limitations and achievable quality of 3D data survey results in such environment is crucial for ensuring the reliability of entire optimization process.

2. MOBILE MAPPING SOLUTIONS IN UNDERGROUND SCENARIOS

2.1 Related works

The issue of assessing accuracy of 3D point clouds for ensuring their suitability for the further analysis has been raised multiple times and for various use cases. Farella (2016) examined a commercial SLAM solution accuracy in the narrow underground corridors using targets measured with a total station. Toschi et al. (2015) performed an in-depth statistical analysis of accuracy of a mobile mapping system, mounted on a car, utilizing ground truth data obtained with a TLS and photogrammetry. Nocerino et al. (2017) similarly examined selected commercial SLAM solutions (a backpack and a handheld scanner) through point cloud comparison with a TLS ground truth data. The tests were performed in indoor and outdoor urban conditions. Lehtola et al. (2017) introduced a multi-scale error metrics for assessing the accuracy of point cloud data and performed the evaluation of multiple SLAM systems in the indoor setting. The works underlines the need of multi-objective 3D data quality

examination for SLAM besides carrying out a raw comparison of geometrical compliance with the reference data. Raval et al. (2019) investigated the ZebRevo SLAM-based mobile mapping system in an underground coal environment to evaluate its potential and identify related challenge. Kim and Choi (2021) proposed an autonomous driving robot to perform 3D mapping of mining tunnels based on two 2D LiDARs placed horizontally and vertically.

2.2 Study area

The test measurements were carried out in the Gontowa adit[1], located in the Owl Mountains in Poland (Figure 1). The tunnels had been carved in sandstone during the World War II by Germans in the scope of the Riese project. Due to several collapses, the site is characterized by irregular geometry, thus being a perfect site to test the performances of mobile mapping units in a complex, uneven, underground scenario.
For the assessment of the SLAM systems (Section 2.3), a part of the surveyed tunnels with a loop shape is considered (ca 120 m in total). This allowed to better check the results of LiDAR odometry, testing the ability of SLAM algorithms to detect loop closures and appropriately adjust the trajectory with a pose graph optimization.

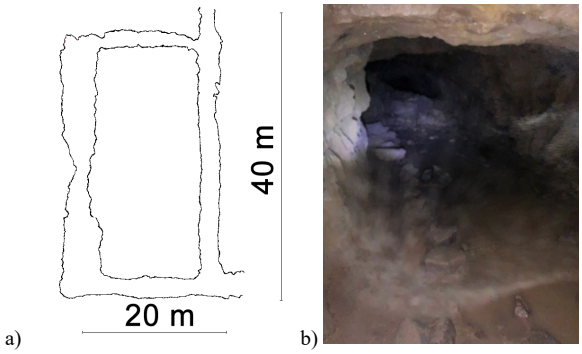

Figure 1: Sketch (a) and a photo (b) of the surveyed tunnel.

2.3 Assessed LiDAR-based mobile mapping systems

Three portable mobile mapping solutions (Table 1) were used during a measurement session in the tunnels:

- a GeoSLAM ZEB Horizon;
- a Livox Horizon LiDAR, coupled with an internal inertial measurement unit (IMU) manually carried during the surveying operations;
- a Velodyne VLP-16 LIDAR sensor coupled with a Dynamixel servomotor.

The Velodyne LiDAR was assembled using open-source libraries and 3D printing rapid prototyping to realized handheld SLAM system (Figure 2a). It was designed for low-cost, fast mapping of unstructured underground environments. Thanks to integration with Robot Operating System (ROS, Quigley et al., 2009), our system is capable of utilizing different SLAM frameworks for LiDAR data, integrating various sources of LiDAR odometry, point cloud ego-motion compensation caused by the LiDAR and actuator rotating motions, as well as online and offline loop closure detection and pose graph optimization. Standardized setup in the ROS environment, using state-of-the-art libraries for point cloud processing and SLAM, such as PCL (Rusu and Cousins, 2011) and GTSAM (Dellaert et al., 2022), allows easy further extensions and improvements or streamlined implementation on a different machine. The setup does not require IMU unit for mapping, which allows to perform mapping tasks even in high-vibration, industrial areas. However, it comes at a cost of expected slight degradation in mapping quality, comparing to LiDAR-inertial solutions.

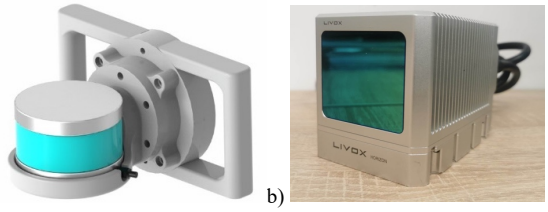

Figure 2: Assessed low-cost LiDAR SLAM systems: in-house 3D design of an actuated Velodyne (a) and a Livox Horizon with an integrated IMU (b).

Sensor	***Sensor parameter***		
	Measurement speed [pts/s]	*Maximum range [m]*	*Ranging accuracy [mm]*
Riegl VZ-400i	500,000	800	5 (@100 m)
GeoSLAM Zeb Horizon	300,000	100	30 (@100 m)
Velodyne VLP-16	300,000	100	30 (@100 m)
Livox Horizon	240,000	90	20 (@25 m)

Table 1: Specification of sensors involved in the study.

2.4 Ground truth data

A dense reference point cloud was acquired with a Riegl VZ-400i TLS, a survey-grade instrument characterized by the ranging precision of 3 mm and accuracy of 5 mm at 100 m distance. First, a field reconnaissance was conducted. The condition and accessibility of the site were assessed and a measurement plan has been prepared. Numerous collapses located mainly at the intersections of the corridors and tight constrictions made the measurements with a heavy TLS significantly more arduous and demanding. Finally, the entire 3D surveying was performed from 60 stations, with the average distance between them being approximately 5 meters. Data acquisition parameters were selected to obtain a scanning grid with a resolution of 9 mm at a distance of 10 m. More than 931 mil points were collected in the entire underground area.
The registration of the 60 individual scans into a single coherent poit cloud was performed with the proprietary RiSCAN PRO software. The employed scans adjustment method is based on plane-to-plane matching of patches extracted from the point clouds, utilizing a solver with a robust kernel. To create the final registered point cloud (Figure 3), some 171,197 patches were used and the final standard deviation of the adjustment was 2.6 mm. The histogram of residuals, indicating their well-balanced, normal distribution, is shown in Figure 4.

Figure 3: Registered reference point cloud of the entire underground complex.

[1] from Latin aditus, entrance

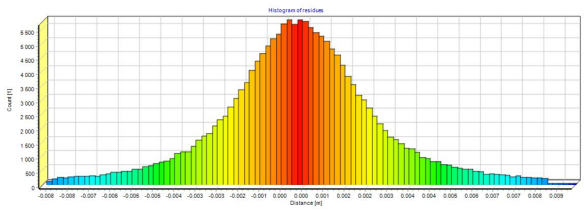

Figure 4: Residual distribution of plane-to-plane TLS point clouds registration.

Finally, cropping to the investigated area of interest and subsampling the point cloud to the maximum resolution of 1 mm, the reference dataset size was reduced to some 11 mil points.

2.5 3D data quality evaluation

The assessment of the 3D reconstruction quality can be performed with a focus on particular aspects of the generated 3D data properties. The most important ones are accuracy (i.e., compliance with the ground truth geometry), completeness (a measure of the area of interest coverage) and precision (point dispersion around the averaged location of a mapped object in a 3D space). Nevertheless, abovementioned qualities are still only a simplification of the broad topic and more metrics have been proposed and analyzed in other works (Lehtola et al., 2017; Trybała et al., 2023).

For analyzing datasets acquired both with photogrammetric (Knapitsch et al., 2017) and laser scanning (Schops et al., 2017) methods, common multi-scale metrics of accuracy and completeness are often used (Nocerino et al., 2017). They derive from the classical metrics of precision and recall in classification problems. The ratio of evaluated points aligned to a ground truth model is calculated at different distance thresholds for determining the precision curve shape. On the contrary, completeness is estimated by thresholding the closest distances calculated from reference data to the analyzed point cloud. Different approaches of estimating the precision metric can be found in the literature, with the calculation of the roughness parameter (Santos and Júlio, 2013) and checking the standard deviation of the least-square fit on the planar surfaces (Chen et al., 2018) being the prevailing options. In this paper, due to lack or regular shapes in the underground tunnel, local accuracy, i.e., quality of the 3D data alignment to the reference data calculated for a small subset of points, will be considered as an approximation of precision evaluation.

However, while being appropriate for tasks of small scenes or object 3D reconstruction, the evaluation of the completeness of large-scale indoor mapping can be heavily influenced by the drift error of the SLAM algorithm. The illustration of this problem is shown in Figure 5: although the point cloud acquired with SLAM is topologically correct, the drift errors result in the global shift of the location of the tunnel on the left side of the figure. While the inclusion of this drift error in assessing the point cloud global accuracy is desired, for estimating completeness it can falsely negatively skew the results. A simple co-registration of the evaluated point cloud with the ground truth data, even using a 9-parameter transform, would not solve the issue, since the rotational and translational errors of the SLAM algorithm cannot be expected to accumulate uniformly with the traveled distance, especially in variable and challenging underground conditions. A method of non-rigid and non-uniform point cloud alignment is needed to obtain an accurate fit to the reference data and calculate an accurate completeness metric (Figure 5b).

To tackle this issue, we propose a sequential, voxel-based adjustment method. Its overview is presented in Figure 6.

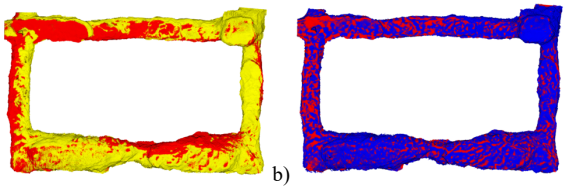

a) b)

Figure 5: Top view of the point clouds depicting the influence of the global drift on their relative alignment: ground truth (red) overlapped with the original Velodyne SLAM data (yellow) (a) and with its drift-compensated version (blue) (b).

First, we downsample the point clouds and create a common voxel grid for all of the evaluated datasets and the ground truth. We then create voxel models, checking the occupancy of each cell with a set minimum threshold of points to minimize the influence of noisy data. Afterward, we start an iterative process of aligning points inside of each voxel to the ground truth with the iterative closest point algorithm (ICP, Rusinkiewicz & Levoy, 2001), estimating the rotation and translation parameters. We select the initial voxel, e.g., the one populated with the highest number of points, and continue aligning subsequent neighboring voxels until all are transformed. We start the alignments with the initial guesses of the transform based on already calculated transforms of the neighboring voxels, which in turn reduces the drift error of the SLAM algorithm. Finally, all points from the original point cloud are transformed according to the transformation of their parent voxel.

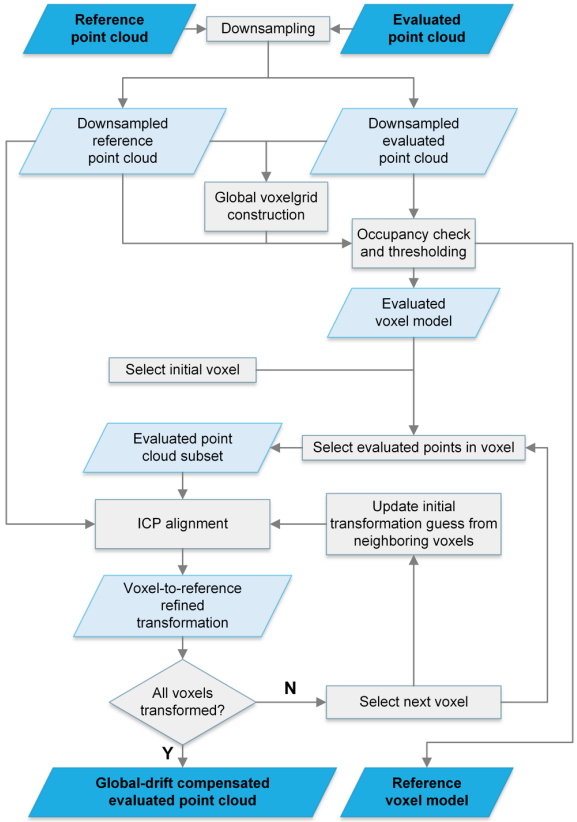

Figure 6: Flowchart of the proposed method for compensating SLAM drift errors and improve the 3D data completeness evaluation.

In our method, we divide the analyzed point clouds regularly in the space domain, i.e., in a voxel grid. Alternatively, a temporal division approach can be used, as presented by Al-Durgham et al. (2021). Nevertheless, this would require the evaluated point clouds to be timestamped or to have the estimated sensor

trajectory with poses corresponding to raw point clouds. This cannot be always achieved, especially with commercial SLAM solutions.
Our approach allows to adjust a whole, single point cloud for the evaluation, without any information on the sensor trajectory, and without artificially reducing the local noise of the point cloud for obtaining accurate completeness and local accuracy estimates.
However, it must be stressed that the presented method does not aim to reduce the SLAM algorithm drift for achieving better mapping results since it utilizes the usually unavailable ground truth data. The presented workflow aims only to improve the process of evaluating the quality of the results obtained with different mobile mapping methods on a test field with reliable reference data.

2.6 Selected metrics

In this case study, results of mapping the underground site with 3 mobile mapping systems are divided into 3 aspects:

a) global accuracy,
b) local accuracy,
c) completeness.

For assessing global and local accuracy, evaluated point clouds registered with a rigid ICP transform to the reference data were used. Global accuracy has been analyzed both using traditional approach (i.e., as percentage of cloud-to-reference unsigned distances below different thresholds) and calculating cloud-to-reference signed distances with M3C2 method available in Cloud Compare software (Lague et al., 2013). Local accuracy has been analyzed through calculating standard deviations of point cloud subset fit in 2 selected areas and 2 cross-sections of the tunnel shown in Figure 7. Completeness metrics has been obtained with point clouds adjusted according to the previously described algorithm, summarized in Figure 6.

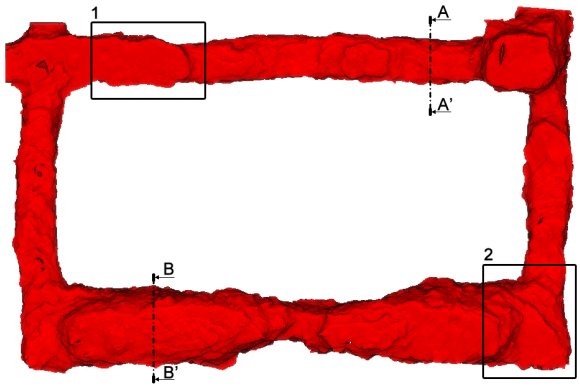

Figure 7: The ground truth point cloud with highlighted regions-of-interest (ROIs) and cross-sections chosen for the selective local accuracy analysis.

3. RESULTS

The SC-LiDAR-SLAM open-source framework (Kim et al., 2022) was adopted for processing the collected LiDAR data. A-LOAM was used as a source of LiDAR odometry for Velodyne and FAST-LIO was selected for Livox. Processing pipelines for both sensors utilized Scan Context++ for loop closure detection and GTSAM for constructing the pose graph. The data collected with the ZEB Horizon were processed with the GeoSLAM proprietary tool.
The perspective views of the resulting point clouds are presented in Figure 8 whereas Figure 9 shows closeup views in one of the more challenging areas, where a passage through the tunnel is steep and narrow due to the rockfall. From those figures onwards, the uniform color coding is kept consistent for all point cloud data, unless indicated otherwise: TLS data is represented in red, GeoSLAM in orange, Velodyne in blue and Livox in green.

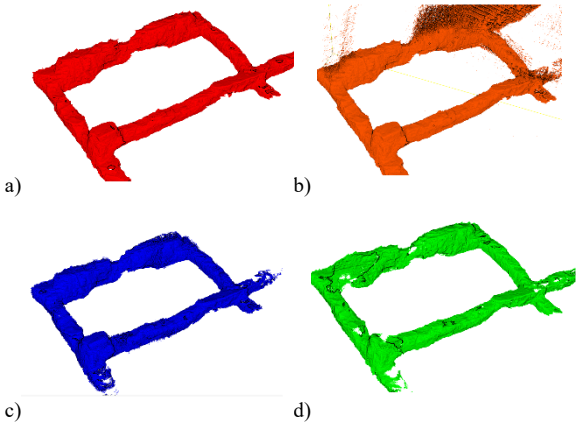

Figure 8: Registered point clouds of the study area: TLS (a), GeoSLAM (b), actuated Velodyne (c) and Livox (d).

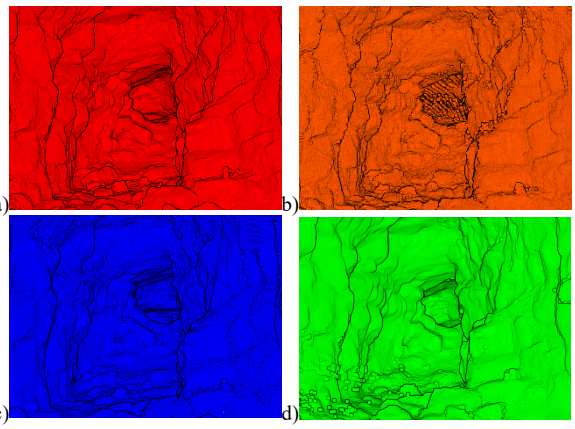

Figure 9: Close view of the collected point clouds of an area with a partly collapsed passage: TLS (a), GeoSLAM (b), actuated Velodyne (c) and Livox (d).

A qualitative investigation of those visualizations reveals some issues with the performance of different tested mapping systems. First, the point cloud from GeoSLAM contains heavy noise, concentrated around the area with the narrow passage of the tunnel. Livox point cloud seems to show the least surface deviation. However, sparse, more apparent erroneous point groups are also visible. The limited field of view of the sensor also caused the presence of visible gaps in the mapping coverage of the tight tunnel spaces. On the other hand, the 3D reconstruction from the actuated Velodyne measurements manifests visibly higher, although more uniformly distributed noise on the surfaces.
In the next step, a quantitative assessment based on metrics selected in Section 2.6 has been performed. First, the local geometry of the mapped areas was examined on the basis of 2 cross-sections and 2 ROIs. Point cloud subsets were registered to the corresponding TLS subset with an ICP algorithm again. This step refines their alignment to the reference data, enabling analyzing the local accuracy of results acquired with tested mapping systems. The resulting aligned point cloud cross-sections and ROIs are shown in Figures 10 and 11, respectively. The standard deviations of each fit are reported in Table 2.

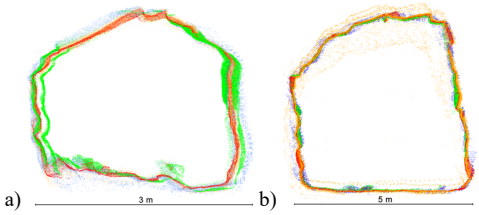

Figure 10: Cross-sections A-A' (a) and B-B' (b) of point clouds acquired with: TLS (red), GeoSLAM (orange), actuated Velodyne (blue) and Livox (green).

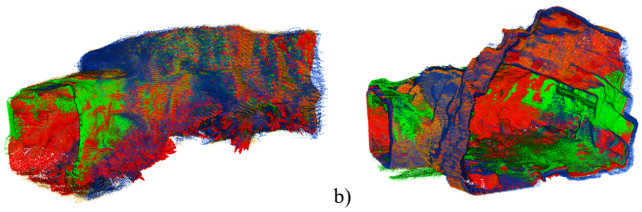

Figure 11: Regions-of-interest (ROIs) No. 1 (a) and No. 2 (b) of point clouds acquired with: TLS (red), GeoSLAM (orange), actuated Velodyne (blue) and Livox (green).

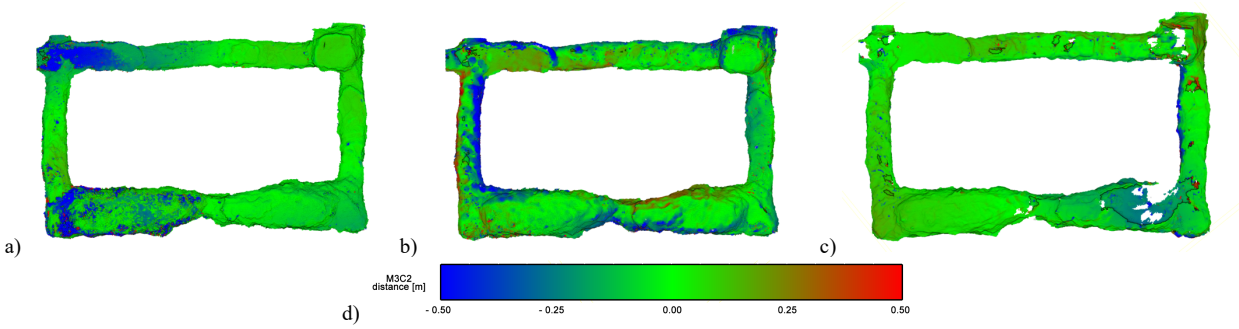

Figure 12: M3C2 signed distances between the ground truth point cloud and GeoSLAM (a), actuated Velodyne (b) and Livox (c) data. Common coloring scheme according to the distance values applied to all point clouds (d).

Sensor	***M3C2 distance σ [mm]***	***Cross-section ICP fit σ [mm]***		***ROI ICP fit σ [mm]***	
		A-A'	*B-B'*	*No.1*	*No.2*
GeoSLAM	364	26	94	49	35
Actuated Velodyne	281	62	59	86	57
Livox Horizon	232	53	24	26	114

Table 2: Standard deviations of comparisons to the ground truth using the entire evaluated datasets (M3C2) and only selected cross-sections and ROIs.

Most notably, a double-wall and double-floor errors is visible for Livox point cloud slice A-A' and ROI No. 2. GeoSLAM exhibits a significantly higher noise level in slice B-B'. Velodyne point cloud fit errors are consistent at a medium level, ranging from 57 to 86 mm. Results from fitting both Livox and GeoSLAM 3D data display higher variability, reaching error extremes from 24 mm to around 100 mm.

Global accuracy was investigated thereafter. Signed distances between each evaluated point cloud were computed and visualized with a common color scheme in Figure 12 to pinpoint the areas of the degradation of the mapping quality due to the drift of the SLAM algorithm. 3D data generated with all mobile mapping systems contain outlier groups in different areas. For the GeoSLAM, they are concentrated in tunnel parts on the left side of Figure 12a, while for the Livox highest error values were estimated for the area on the right side of the Figure 12c. Velodyne point cloud, presented in Figure 12b, differs from the ground truth mostly in the lower and left part of the figures. All of the examined SLAM variations exceeded the standard deviation of the signed distances to the reference data of 200 mm (Table 2). However, this not necessarily indicate the bad quality of the mapping results, but only the expected presence of the drift error since no global positioning source was available in the underground site. This results in numerous groups of outlying points (in terms of global accuracy), which on purpose were not manually removed or corrected. This is further proved by degradation of global accuracy concentrated in the in the lower left corner of the figure: the area furthest from the mapping starting point (and thus, the loop closure location).

Another aspect of 3D data quality assessment, the completeness, was studied with drift-compensated versions of all evaluated point clouds. However, to showcase the difference between our proposed approach and the original, completeness curves were approximated and plotted with both methods (Figure 13). Noticeable difference can be seen not only in the absolute values, but also in the shape of the curves, indicating that our method provides estimates of the completeness metric in a more reliable and accurate manner.

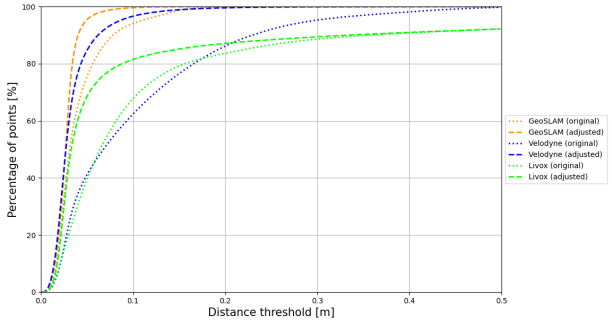

Figure 13: Comparison of completeness curves calculated for the analyzed datasets with the original method and our approach.

Furthermore, accuracy and completeness curves, calculated as described in Section 2.6, are presented in Figure 14. The plot summarized the weaknesses of each tested method. Completeness of Velodyne and GeoSLAM mapping results quickly reaches values close to 100%. The accuracy of GeoSLAM, matching the Livox accuracy for low distance thresholds, plateaus at around 95% due to the presence of highly erroneous points.

On the other hand, Velodyne's accuracy rises considerably slower, but consistently, to almost 100% at the 0.5 m threshold. 3D data generated with Livox achieves superior accuracy of all the tested methods, but due to narrow field of view, its results show an impaired completeness of the measurements even at high distance thresholds.

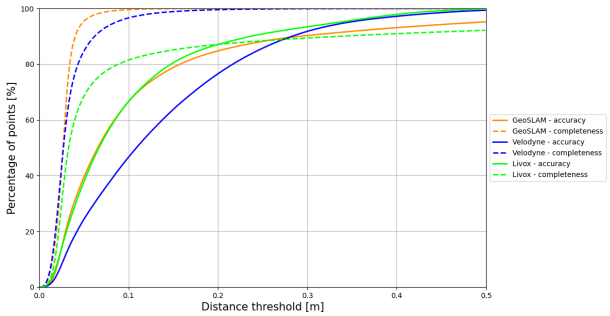

Figure 14: Resulting estimates of accuracy and adjusted completeness for different distance thresholds for the evaluated SLAM point clouds.

To easily visualize the spatial distribution of areas with lower completeness and local accuracy, a simple voxel-based comparison method was developed. Using the common voxel grid, prepared during the drift-compensation phase of data processing, we compare the occupancy of voxels in each examined model with the reference voxel model. Thus, true positive (*TP*) voxel is occupied both in the examined and the ground truth data; false negative (*FN*) voxel is occupied only in the reference model, and a false positive (*FP*) voxel corresponds to a voxel occupied only in the evaluated dataset. Their percentages have been calculated for 2 voxel sizes (0.2 m and 0.5 m) and listed in Table 3 and the corresponding visualizations are included in Figure 15. Confirming the findings of previous analyzes, the number of incorrectly mapped voxels for GeoSLAM and the number of unmapped voxels for Livox stay high even at lower resolutions, while results from Velodyne scanning generally improve in all aspects.

System	***20 cm voxel count [%]***			***50 cm voxel count [%]***		
	TP	*FN*	*FP*	*TP*	*FN*	*FP*
GeoSLAM	61	3	36	82	1	17
Actuated Velodyne	57	25	18	88	5	7
Livox Horizon	49	30	21	74	18	8

Table 3: Ratios of voxels classified according to their occupancy compared to the reference voxel model.

4. CONCLUSIONS

This study presented a comprehensive assessment of the quality of results obtained from different 3D LiDAR-based mobile mapping techniques in an underground environment. We presented 2 in-house built systems, based on popular low-cost 3D LiDAR sensors, manufactured by Velodyne and Livox, and utilizing open-source SLAM frameworks for generating co-registered point clouds. We compared such sensors to the GeoSLAM Zeb Horizon commercial solution and benchmark all systems against reference data collected with survey-grade TLS. Analyzing different aspects of 3D data quality provides insights into the unique strengths and limitations of each examined approach, which need to be considered when selecting the appropriate method for a particular application of 3D reconstruction of complex underground scenes.

Based on our findings and the presented comparison methodology, an optimal mobile mapping system can be chosen according to the desired focus on the particular 3D data quality: accuracy and completeness. A crucial aspect is the determination of their critical values for selected metrics representing them. For example, for the VOT3D project purposes and ventilation simulations at a large scale, systems maximizing the completeness of the measurements, i.e., GeoSLAM and our actuated Velodyne system, would be the most suitable options. While the former has the potential to achieve greater accuracy, the latter might provide more robustness in the industrial mine environment due to not utilizing inertial data. On the other hand, applications requiring high accuracy and providing more room for maneuvering the sensor could benefit from employing a Livox-based mobile mapping system.

The article reported also a dedicated technique for improving the assessment of 3D reconstruction completeness through applying an iterative, voxelized ICP alignment refinement. The proposed method aims to provide a more accurate assessment of real coverage of the 3D scene, obtained with SLAM. We reduced the influence of one of its inherent error sources, the drift, on the resulting completeness estimate. The approach is designed to be versatile due to the fact of requiring only the 3D point cloud data (reference and assessed) as the input.

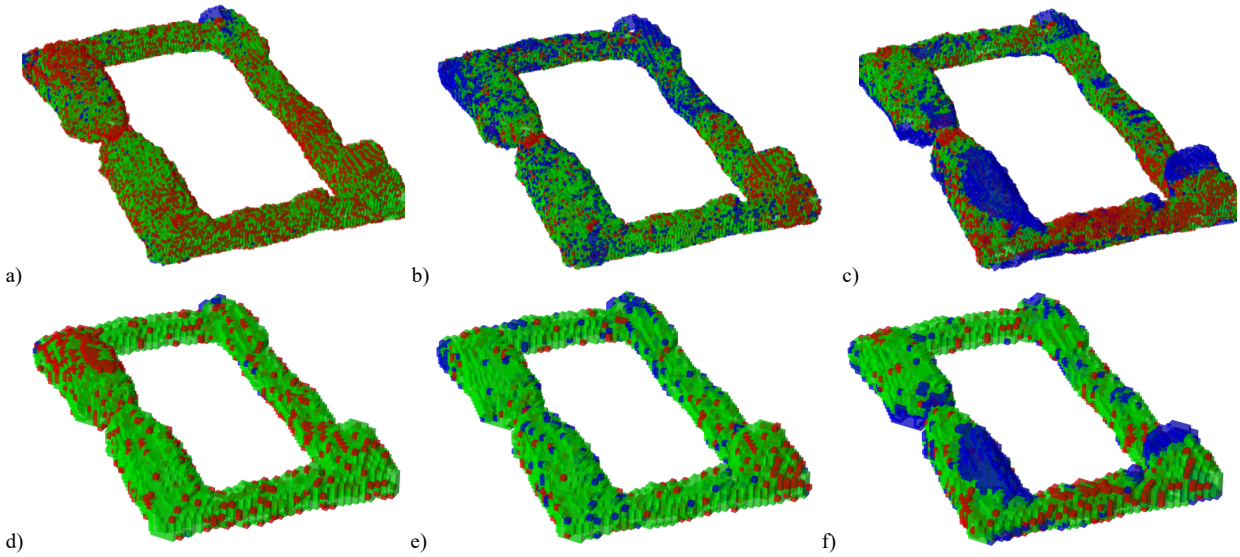

Figure 15: 3D visualizations of the voxel-based point cloud comparison with the reference data: GeoSLAM (a, d), actuated Velodyne (b, e) and Livox (c, f). Voxels compliant with the ground truth data are shown in green, non-mapped areas in blue and incorrect voxels in red. Figures a-c rendered for 0.2 m voxel size, figures d-f for 0.5 m voxel size.

ACKNOWLEDGEMENTS

This work has been party supported by the EIT-RM project VOT3D - Ventilation Optimizing Technology based on 3D-scanning (https://vot-3d.com/).

REFERENCES

Al-Durgham, K., Lichti, D. D., Kwak, E., & Dixon, R., 2021. Automated accuracy assessment of a mobile mapping system with lightweight laser scanning and MEMS sensors. *Applied Sciences*, 11(3), 1007.

Chen, J., Mora, O. E., & Clarke, K. C., 2018. Assessing the accuracy and precision of imperfect point clouds for 3d indoor mapping and modeling. *Int. Ann. Photogramm. Remote Sens. Spatial Inf. Sci.*, 4, pp. 3-10.

Dellaert, F. & GTSAM Contributors, 2022. *Borglab/GTSAM*. 4.2a8, Georgia Tech Borg Lab.

Di Stefano, F., Torresani, A., Farella, E. M., Pierdicca, R., Menna, F., Remondino, F., 2021. 3D surveying of underground built heritage: Opportunities and challenges of mobile technologies. *Sustainability*, 13(23), 13289.

Ebadi, K., Bernreiter, L., Biggie, H., Catt, G., Chang, Y., Chatterjee, A., Denniston, C. E., Deschênes, S.-P., Harlow, K., Khattak, S., Nogueira, L., Palieri, M., Petráček, P., Petrlík, M., Reinke, A., Krátký, V., Zhao, S., Agha-mohammadi, A., Alexis, K., Carlone, L., 2022. Present and future of SLAM in extreme underground environments. *arXiv preprint* arXiv:2208.01787.

Elhashash, M., Albanwan, H., Qin, R., 2022. A review of mobile mapping systems: from sensors to applications. *Sensors*, 22, 4262.

Farella, E. M., 2016. 3D mapping of underground environments with a hand-held laser scanner. *Bollettino della società italiana di fotogrammetria e topografia (SIFET)*, (2), pp. 1-10.

Kim, G., Yun, S., Kim, J. & Kim, A. 2022. SC-LiDAR-SLAM: A Front-end Agnostic Versatile LiDAR SLAM System. *Proc. Int. Conference on Electronics, Information and Communication* (ICEIC), pp. 1-6.

Kim, H., Choi, Y., 2021. Location estimation of autonomous driving robot and 3D tunnel mapping in underground mines using pattern matched LiDAR sequential images. *International Journal of Mining Science and Technology*, 31(5), pp. 779-788.

Knapitsch, A., Park, J., Zhou, Q.Y., Koltun, V., 2017. Tanks and temples: Benchmarking large-scale scene reconstruction. *ACM Trans. Graph. ToG*. 36, pp. 1–3.

Jones, E.W., 2020. Mobile LiDAR for underground geomechanics: learnings from the teens and directions for the twenties. Proc. 2nd *UMT Conference*, pp. 3-26.

Lague, D., Brodu, N., & Leroux, J., 2013. Accurate 3D comparison of complex topography with terrestrial laser scanner: Application to the Rangitikei canyon (NZ*). ISPRS journal of photogrammetry and remote sensing*, 82, pp. 10-26.

Lehtola, V. V., Kaartinen, H., Nüchter, A., Kaijaluoto, R., Kukko, A., Litkey, P., Hyyppä, J., 2017. Comparison of the selected state-of-the-art 3D indoor scanning and point cloud generation methods. *Remote sensing*, 9(8), 796.

Liang, X., Hyyppa, J., Kukko, A., Kaartinen, H., Jaakkola, A., Yu, X., 2014. The use of a mobile laser scanning system for mapping large forest plots. *IEEE Geosci. Remote Sens. Lett.*, *11*, pp. 1504-1508.

Menna, F., Torresani, A., Battisti, R., Nocerino, E., Remondino, F., 2022: A modular and low-cost portable VSLAM system for real-time 3D mapping: from indoor and outdoor spaces to underwater environments. *Int. Arch. Photogramm. Remote Sens. Spatial Inf. Sci.,* XLVIII-2/W1-2022, pp. 153-162.

Nocerino, E., Menna, F., Remondino, F., Toschi, I., & Rodríguez-Gonzálvez, P., 2017. Investigation of indoor and outdoor performance of two portable mobile mapping systems. In *SPIE Videometrics, Range Imaging, and Applications XIV,* Vol. 10332, pp. 125-139.

Nocerino, E., Rodríguez-Gonzálvez, P. and Menna, F., 2019. Introduction to mobile mapping with portable systems. In Laser Scanning: *An Emerging Technology in Structural Engineering*. In Laser Scanning - An Emerging Technology in Structural Engineering, Chapter 4, CRC Press.

Nocerino, E., Stathopoulou, E. K., Rigon, S., & Remondino, F., 2020. Surface reconstruction assessment in photogrammetric applications. *Sensors*, 20(20), 5863.

Otero, R., Lagüela, S., Garrido, I., Arias, P., 2020. Mobile indoor mapping technologies: A review. *Automation in Construction*, Vol. 120, 103399.

Perfetti, L. and Fassi, F., 2022. Handheld fisheye multicamera system: surveying meandering architectonic spaces in open-loop mode – accuracy assessment. *Int. Arch. Photogramm. Remote Sens. Spatial Inf. Sci.,* XLVI-2/W1-2022, pp. 435-442.

Pierzchała, M., Giguère, P., Astrup, R., 2018. Mapping forests using an unmanned ground vehicle with 3D LiDAR and graph-SLAM. *Computers and Electronics in Agriculture*, 145, pp. 217-225.

Quigley, M., Conley, K., Gerkey, B., Faust, J., Foote, T., Leibs, J., Berger, E., Wheeler, R., Ng, A.Y., 2009. ROS: an open-source robot operating system. *In Proceedings of the ICRA Workshop on Open Source Software,* Vol. 3, pp. 5.

Raval, Banerjee, B.P., Kumar Singh, S., Canbulat, I., 2019. A preliminary investigation of mobile mapping technology for underground mining. Proc. *IEEE IGARSS*, pp. 6071-6074.

Rusinkiewicz, S., & Levoy, M., 2001. Efficient variants of the ICP algorithm. Proc. 3rd *3DIM Conference*, pp. 145-152.

Rusu, R.B., Cousins, S., 2011. 3D is here: Point Cloud Library (PCL). Proc. *IEEE Int. Conference on Robotics and Automation*, pp. 1-4.

Santos, P.M., Júlio, E.N., 2013. A state-of-the-art review on roughness quantification methods for concrete surfaces. *Construct. Build. Mater.*, 38, pp. 912–923.

Schops, T., Schonberger, J.L., Galliani, S., Sattler, T., Schindler, K., Pollefeys, M., Geiger, A., 2017. A multi-view stereo

benchmark with high-resolution images and multi-camera videos. Proc. *CVPR.*

Toschi, I., Rodríguez-Gonzálvez, P., Remondino, F., Minto, S., Orlandini, S., Fuller, A., 2015. Accuracy evaluation of a mobile mapping system with advanced statistical methods. *Int. Arch. Photogramm. Remote Sens. Spatial Inf. Sci.*, 40(5), 245.

Trybała, P., Szrek, J., Remondino, F., Wodecki, J., Zimroz, R., 2022: Calibration of a multi-sensor wheeled robot for the 3d mapping of underground mining tunnels. *Int. Arch. Photogramm. Remote Sens. Spatial Inf. Sci.,* XLVIII-2/W2-2022, pp. 135-142.

Trybała, P., Szrek, J., Dębogórski, B., Ziętek, B., Blachowski, J., Wodecki, J., & Zimroz, R., 2023. Analysis of Lidar Actuator System Influence on the Quality of Dense 3D Point Cloud Obtained with SLAM. *Sensors*, 23(2), 721.

Xie, Y., Yang, T., Wang, X., Chen, X., Pang, S., Hu, J., Wang, A., Chen, L., Shen, Z., 2022. Applying a portable backpack LiDAR to measure and locate trees in a nature forest plot: accuracy and error analyses. *Remote Sensing*, *14*, 1806.